IEEE Access
Multidisciplinary | Rapid Review | Open Access Journal

Received February 1, 2020, accepted February 14, 2020, date of publication February 18, 2020, date of current version February 27, 2020.

Digital Object Identifier 10.1109/ACCESS.2020.2974765

Optimization Research on a Switching Power Amplifier and a Current Control Strategy of Active Magnetic Bearing

YAPING HE[1,2], XI HE[2], JIEN MA[1], AND YOUTONG FANG[1]
[1]College of Electrical Engineering, Zhejiang University, Hangzhou 310000, China
[2]Zhuzhou CRRC Times Electric Co., Ltd., Zhuzhou 412001, China

Corresponding author: Yaping He (hexihnu@foxmail.com)

This work was supported in part by the National Natural Science Foundation of China under Grant 51637009 and Grant 51827810.

ABSTRACT Active magnetic suspension bearing technology has been widely used in the field of high-speed motors because of its many technical advantages. A switching power amplifier is an important part of active magnetic bearing. This paper first analyzes the topology of a switching power amplifier and proposes an optimized switching power amplifier topology, which can significantly reduce the number of switches used in a power amplifier. Then, by studying the transfer function of the system, the boundary conditions of the power amplifier bandwidth, stiffness and damping, which maintain system stability, are obtained. Furthermore, an improved current control strategy is proposed, and this strategy can significantly improve the bandwidth of the switching power amplifier and improve the stability and dynamic performance of the system. Simulations and experiments verify the practicability and effectiveness of the topology and current control strategy proposed in this paper.

INDEX TERMS Active magnetic bearing, switching power amplifier, control bandwidth.

I. INTRODUCTION

Electromagnetic levitation technology has been widely studied since its invention [1]. This technology was first used in magnetic levitation trains and then gradually applied to the field of motor bearings [2]. A motor bearing with active magnetic suspension technology can place the rotor of the motor in a suspension state, providing a magnetic suspension motor with excellent characteristics, such as no contact, no lubrication and no wear. To date, magnetic levitation motors have been widely used in medical equipment, turbine machinery and other fields [3] and have been favored in industrial applications.

Fig. 1 shows a structure diagram of a active magnetic bearing, which is composed of a front radial bearing, a rear radial bearing and an axial bearing. The motor rotor and the thrust plate are located in the middle of the bearing. The bearing consists of a magnetic coil. Each radial magnetic bearing controls the rotor's 2 axes of radial direction in the bearing plane, and the axial magnetic bearing controls the rotor's axial direction. For each axis, two coils form a set of differential coils for control. For a 5-axis magnetic bearing system, a total of 10 coils need to be accessed to achieve control.

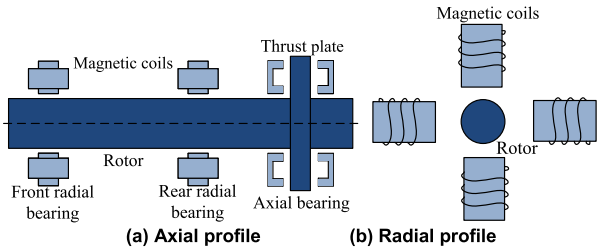

FIGURE 1. Structural diagram of active magnetic bearing.

A schematic diagram of single-axis differential control is shown in Fig. 2. The electromagnetic force of an active magnetic bearing is determined by the position of the rotor, the offset current and the differential current. In an actual control process, the electromagnetic force can be controlled by regulating the difference current, and then the rotor position can be controlled.

The associate editor coordinating the review of this manuscript and approving it for publication was Alexander Micallef.

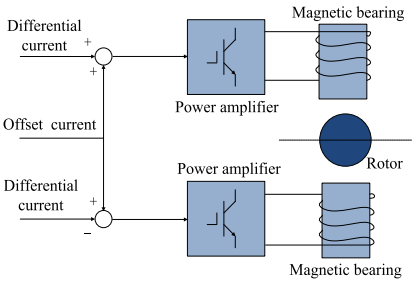

FIGURE 2. A magnetic bearing differential control.

A power amplifier is an important part of the control mechanism. Linear power amplifiers and switching power amplifiers are the two types of power amplifier circuits applied in electromagnetic systems. Linear power amplifiers are rarely used in high-power and current systems due to their inherent large loss defects [4]. Therefore, switching power amplifiers are commonly used in magnetic suspension bearing control systems. There are numerous studies in the literature on magnetic bearing switching power amplifiers [5]–[8]. A five-phase six-leg switching power amplifier was designed in [5] that is characterized by small size and simple control. In addition, a novel converter topology for a magnetic bearing drive was introduced in [8], which can ride through the open-circuit fault of a power electronics switch in operation and maintain levitation for the magnetic bearing. The above article carried out topology optimization to promote device longevity and reliability. However, these aforementioned topology optimizations can be further improved, as the influence of topology optimization on the overall performance of the system was not taken into account.

Considering rotor position control, the system is generally regarded as a mechanical spring-like system with certain stiffness and damping characteristics. In engineering applications, the rotor position can be controlled by a distributed PID control [9]. Many optimized control strategies have been proposed [10]–[20]. [12] adopted a Kalman filter and state feedback control to improve the operational performance of an active magnetic bearing. Reference [16] applied a second-order sliding-mode concepts in an active magnetic bearing. In addition, [19] introduced an intelligent control design that captures the nonlinearity and fuzziness of uncertain magnetic bearing systems. The above papers all focused on the position ring control of the magnetic suspension bearing, but the influence of a switching power amplifier on the stability of a magnetic suspension bearing system and its relationship with the damping and stiffness of the system require further analysis.

In this paper, the control system of active magnetic bearing was studied and optimized. In practical engineering applications, the volume, reliability, running stability, response characteristics and cost of the magnetic suspension control system should be comprehensively considered. Based on these practical engineering applications, comprehensive optimization studies on the active magnetic bearing control system were carried out, including the optimization of the power amplifier topology, an analysis of the relationship between the stable operation control and the inherent characteristics of the system, and improvements to the current control strategy, which can optimize the operation stability and the corresponding characteristics of the active magnetic bearing. Finally, the feasibility of the optimization work was verified via simulations and tests of the active magnetic bearing.

II. SWITCHING POWER AMPLIFIER OF ACTIVE MAGNETIC BEARING

As the driving part of the magnetic bearing, the power amplifier is a device used to convert the control signal into an induction current, thereby generating a magnetic field force to drive the magnetic bearing. The power amplifier is generally composed of power electronic devices. At present, a single H-bridge is commonly used to control each pair of coils, and each coil is controlled independently, as shown in Fig. 3. The main disadvantage of the topology is that there are many power electronics used; e.g., there are 40 switching devices required in a 5-axis system.

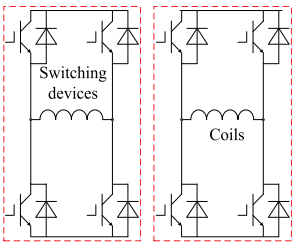

FIGURE 3. An H-bridge switching power amplifier topology.

To reduce the number of power amplifier switching devices, a common bridge and a winding bridge were adopted in this study. One side of all the coils in the 5-axis system was connected to the common bridge, and the other side was connected to the respective winding bridge to form a 5-axis common bridge topology, as shown in Fig. 4. In this topology, 10 induction coils were driven by 22 switching devices, which can reduce the cost of the power amplifier and improve the complexity compared to the H-bridge topology.

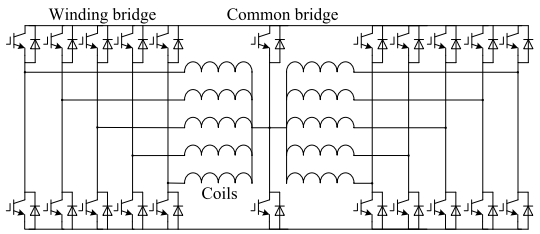

FIGURE 4. A 5-axis common bridge switch power amplifier topology.

In a 5-axis common bridge switch power amplifier topology, there are two current circulation modes, namely, a positive direction mode and a negative direction mode, as shown

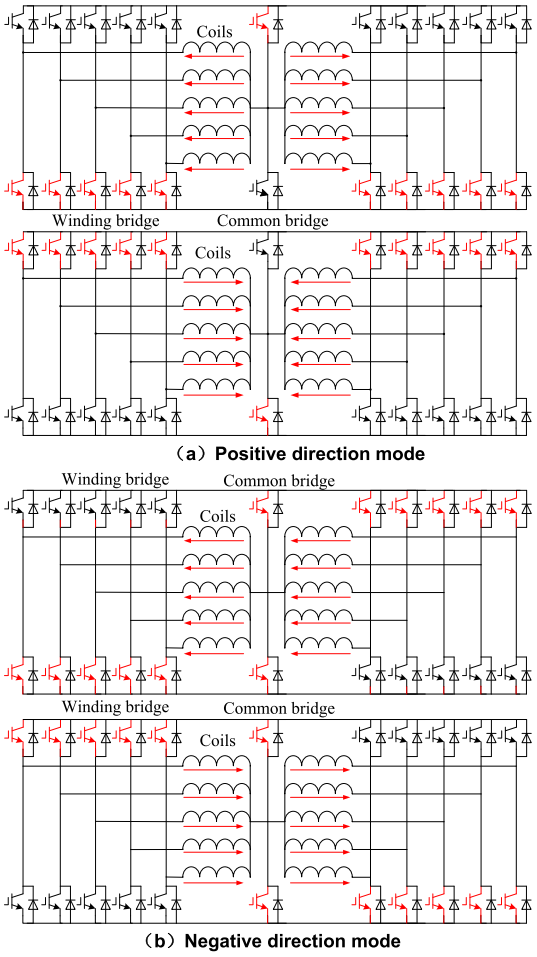

FIGURE 5. Current direction of five-axis common-leg switch power amplifier topology.

in Fig. 5. In the positive direction mode, the upper switch of a winding bridge arm and the lower switch of a common bridge arm (or the lower switch of a winding bridge arm and the upper switch of a common bridge arm) are used to control the inductive current. The current in the common bridge arm is the sum of the current in all winding bridge arms, which will result in high power consumption in the common bridge arm, which is not conducive to the long-term, stable operation of the switching power amplifier. In the negative direction mode, the inductive current is controlled by the upper switch of the left winding bridge arm and the lower switch of the right winding bridge arm (or the lower switch of the left winding bridge arm and the upper switch of the right winding bridge arm). The current in the winding bridge arm will be neutralized at the midpoint of the common bridge arm. The current in the common bridge arm will be small, and the total power consumption of the switching power amplifier will decrease significantly. Therefore, the negative direction mode was adopted in this paper. In addition, in the negative direction mode, the same effect can be achieved with the two types of switching using this method, which can provide redundancy for the power amplifier.

Furthermore, since magnetic suspension bearings are usually controlled by differential currents, the current sum of the two coils of each radial freedom is equal, the coil configuration shown in Fig. 6 can minimize the current in the common bridge arm, which is the current difference between the two coils in the axial direction. In this way, the power loss of the switching power amplifier was decreased by 50% compared with that of the H-bridge topology.

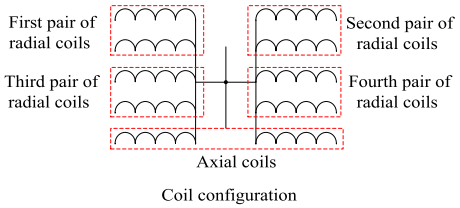

FIGURE 6. Configuration mode of active magnetic bearing coils.

For a further analysis of the on-off situation of the switch, the 5-axis common bridge switch power amplifier can be simplified into a one-axis common bridge, as shown in Fig. 7, where S1∼S6 are switches, and D1∼D6 are diodes.

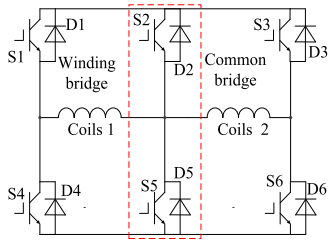

FIGURE 7. Single-axis common bridge switching power amplifier topology.

To independently control the current in each winding, a fixed duty cycle of 50% was set up in the common bridge, and a variable duty cycle, which is opposite to the common bridge, was set up in the winding bridge. When S1 and S5 (S4 and S6) are both turned on, the loop of coil 1 (coil 2) will be under a forward conduction state; when S1 and S5 (S4 and S6) are both turned off, the loop of coil 1 (coil 2) will be under a negative conduction state; when only one of switching devices of the winding bridge and the corresponding common bridge is turned on, the loop will be under a freewheeling state with the current through diode. Certainly, we can use S2 and S4 for coil 1 and use S3 and S5 for coil 2. All of the states are shown in Fig. 8.

III. STABILITY AND CONTROL STRATEGY OF SWITCHING POWER AMPLIFIER

A. TRANSIENT STATE OF SWITCHING POWER AMPLIFIER

The switching power amplifier topology of the active magnetic bearing does not affect the conduction principle. The current in the coil is regulated by the average voltage, which is controlled by the on/off cycles of the switch. In a switching cycle, there are three modes in the switching power amplifier

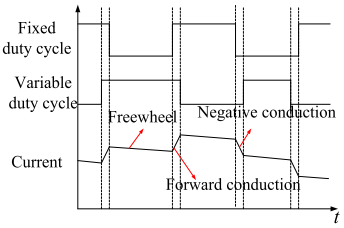

FIGURE 8. Switching state of switching power amplifier.

topology, including forward conduction, freewheeling, and negative conduction, as shown in Fig. 9, where V_{dc} is the voltage on the DC side, L is the coil inductance, R is the coil resistance value, and i_L is the induction current.

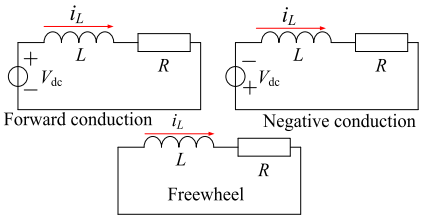

FIGURE 9. Transient state of switching power amplifier.

The forward conduction time ratio was set to c_+, the negative conduction time ratio was set to c-, and the freewheeling time ratio was set to c_0 in a switching cycle of the switching power amplifier. The working state of the loop in one cycle was weighted, and the resulting loop equation was obtained as shown in (1).

$$\begin{aligned} Ri_L + L\frac{di_L}{dt} &= c_+V_{dc} - c_-V_{dc} + c_0 \times 0 \\ &= c_+V_{dc} - c_-V_{dc} \end{aligned} \tag{1}$$

In the formula, c_+ and c- are limited by the selected topology. For H-bridge topology, c_+ and c- have a range of 0∼1; for the common bridge topology, c_+ and c- have a range of 0∼0.5. The maximum values of c_+ and c- were the voltage utilization rates on the DC side.

The voltage utilization rate on the DC side was set to a, and the offset current was set to i_0. The maximum change rate of the current can be obtained in (2), which shows that the change rate of the current was affected by the loop inductance, the positive and negative conduction times, the offset current, and the voltage on the DC side.

$$\max(\frac{di_L}{dt}) = \frac{aV_{dc} - Ri_0}{L} \tag{2}$$

In engineering applications, the offset current and loop resistance are small, so Formula (2) can be simplified as Formula (3).

$$\max(\frac{di_L}{dt}) = \frac{aV_{dc}}{L} \tag{3}$$

As shown in Formula (3), the maximum change rate of the current is limited by the inductance, the voltage on the DC side and its utilization rate.

The response speed of the current is a characteristic of the overall performance of the topology. When the switching topology and the switching drive characteristics are determined, the value can be determined, which means that the max current change rate is only related to the voltage and the inductance. Therefore, when designing an active magnetic bearing system, the coil and the driving voltage should be strictly matched according to the response speed requirement.

B. SYSTEM STABILITY ANALYSIS

A typical control block diagram of a single-axis active magnetic bearing control system is shown in Fig. 10, where x^* is the position reference signal, x is the position output, m is the rotor mass, k_i is the force current coefficient, k_s is the force displacement coefficient, G_{pos} is the position loop control transfer function, G_{cur} is the current loop control transfer function, and G_{PA} is the power amplifier transfer function.

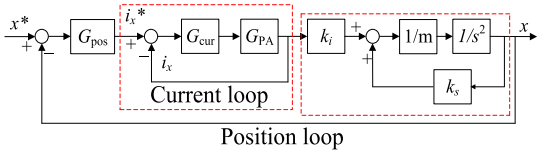

FIGURE 10. Control topology of single-axis system.

PD control is generally adopted for the position loop control transfer function G_{pos}, and its parameter selection is shown in [4], where k is the system stiffness, and D is the system damping.

$$G_{pos} = \frac{k + k_s}{k_i} + \frac{D}{k_i}s \tag{4}$$

The current inner loop was composed of the current control loop G_{cur} and the power amplifier loop G_{PA}, which could be equivalent to an integral loop under a certain bandwidth. The bandwidth was set to ω_c, and the open-loop transfer function of the current loop could be obtained as shown in (5).

$$G_{cur} * G_{PA} = \frac{\omega_c}{s} \tag{5}$$

For the single-axis control block diagram shown in Fig. 7, the closed-loop transfer function can be obtained, as shown in (6).

$$G_C(s) = \frac{G_{pos}G_{cur}G_{PA}k_i}{ms^2 + G_{cur}G_{PA}(ms^2 + G_{pos}k_i + k_s)} \tag{6}$$

(4) and (5) were introduced into the above formula:

$$G_C(s) = \frac{D\omega_c s + (k + k_s)\omega_c}{ms^3 + m\omega_c s^2 + (D\omega_c - k_s)\,s + k\omega_c} \tag{7}$$

The parameters of active magnetic bearing system are shown in Table 1, which are used to analyze the relationship between the current loop bandwidth and system stiffness and the system stability.

When the system stiffness was the natural stiffness ($k = k_s$), the system damping was the critical damping ($D = 2\sqrt{mk}$), and the current loop bandwidth ω_c was

TABLE 1. Active magnetic bearing parameters.

Name	Value
k_s(N/m)	4.3×10^6
k_i(N/A)	2.1×10^3
m(kg)	91.79

changed within the range of 1∼500, the closed-loop pole trajectory of the system occurred as shown in Fig. 11(a). There are three root trajectories, two of which cross the imaginary axis into the right half plane as the current loop bandwidth decreases. This result shows that, given the system stiffness and damping, the system tends to be unstable with the decrease in the current loop bandwidth. Therefore, in order to make the system run steadily, we need enough current loop bandwidth.

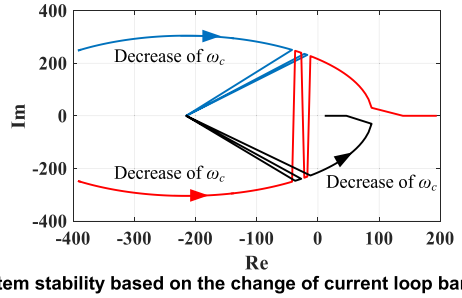

(a) System stability based on the change of current loop bandwidth

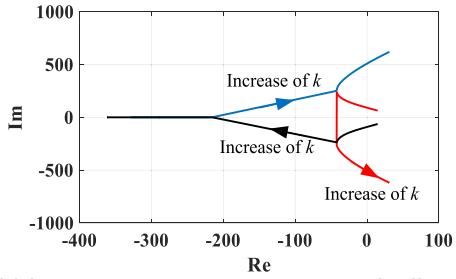

(b) System stability based on the change of stiffness

FIGURE 11. Closed-loop pole trajectory of the system.

When the current loop bandwidth was $\omega_c = 300$, and the system stiffness k was changed within the range of $0.1\sim10k_s$, the closed-loop pole trajectory of the system occurred as shown in Fig. 11(b). When k was too small or too large, there were two root trajectories that crossed the imaginary axis into the right half-plane. This result shows that too little stiffness and too much stiffness will destabilize the system. To make the system stable, we need to select an appropriate stiffness value.

As shown from the above analysis, the current loop bandwidth in engineering applications would limit the system stiffness.

By further analyzing the closed-loop transfer function, the characteristic equation can be obtained as shown in (8).

$$D(s) = ms^3 + m\omega_c s^2 + (D\omega_c - k_s)\, s + k\omega_c \tag{8}$$

Based on Rolls stability criterion, the conditions for stabilizing the system were as follows:

$$m\omega_c\,(D\omega_c - k_s) - mk\omega_c > 0 \tag{9}$$

The above formula was then simplified as follows:

$$\frac{k + k_s}{D\omega_c} < 1 \tag{10}$$

Formula (10) shows the relationships among the stiffness k, the damping D, and the current loop bandwidth ω_c in a stable system; thus, the current loop bandwidth should be greater than $(k + k_s)/D$ to enable the stability of the system. When the system stiffness was the natural stiffness ($k = k_s$), and the system damping was the critical damping ($D = 2\sqrt{mk}$), using the parameter given in Table 1, we could calculate the minimum of ω_c to be 207. In addition, when the system damping D and the current loop bandwidth ω_c were constant, the maximum stiffness of the system was $D\omega_c$-k_s.

C. IMPROVED CURRENT CONTROL STRATEGY

In engineering applications, the current control loop G_{cur} can be designed as a PI controller. Generally, a good effect can be obtained with a current loop formed by a PI controller. As seen in the above section, the active magnetic bearing control system has a high response speed requirement for the current, but a PI controller cannot achieve the maximum response speed of the current loop as shown in (3) due to the limit of its closed-loop adjustment process.

To improve the response speed of the current control loop, a current inner loop control method based on the model prediction was proposed. First, (1) was discretized as shown in (11).

$$cV_{dc} = L\frac{(i_{k+1} - i_k)}{T} + R\frac{(i_{k+1} + i_k)}{2} \tag{11}$$

where T is the switching period, c is the time ratio used to access the power supply on the DC side, and i_{k} and $i_{\text{k+1}}$ are the current sampling values in the two adjacent switching cycles.

If the current reference value was set to $i_{\text{k+1}}$, and the current feedback value was set to i_{k}, the value of d required for the next switching cycle could be predicted, as shown in (12).

$$d = L\frac{(i_{k+1} - i_k)}{TV_{dc}} + R\frac{(i_{k+1} + i_k)}{2V_{dc}} \tag{12}$$

With the above formula, the current control strategy based on the model prediction could be obtained. The control block diagram is shown in Fig. 12.

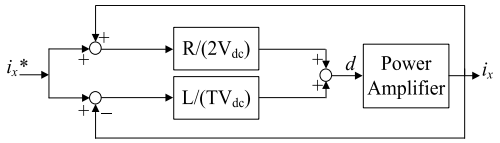

FIGURE 12. Predicted model current control strategy.

IV. SIMULATION AND TEST VERIFICATIONS

A. SIMULATION VERIFICATION

The coil parameters of the active magnetic bearing switching power amplifier studied in this paper are shown in Table 2. The current responses of the different switching power amplifier topologies based on this simulation analysis are shown in Fig. 13. When the current reference value changed from 0 A to 5 A, the H-bridge topology and five-axis common bridge topology could keep up with the current reference value. However, the current response speed of the H-bridge topology was faster than that of the five-axis common bridge topology. This finding is consistent with theoretical analysis.

TABLE 2. Active magnetic bearing switching power amplifier and coil parameters.

Parameter	Value
Voltage on DC side (V)	300
Coil resistance (Ω)	1.32
Coil inductance (H)	0.6825
Rated current (A)	4

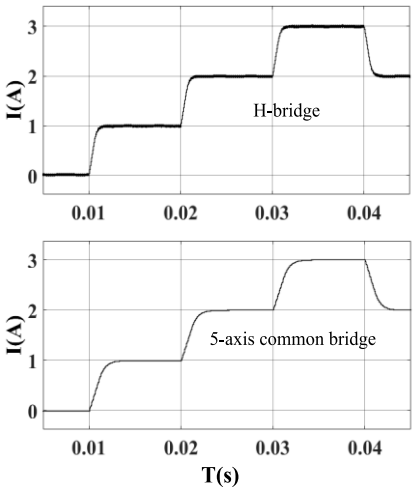

FIGURE 13. Current response speeds at different topologies.

The 5-axis common bridge switching power amplifier topology was selected to simulate and analyze the response characteristics of two different current control modes as shown in Fig. 14. When the current reference value changed from 0 A to 5 A, the current response speed and the control accuracy based on the model prediction control strategy were better than those based on the PI control strategy.

The displacement response characteristics of an active magnetic bearing with two current control modes and

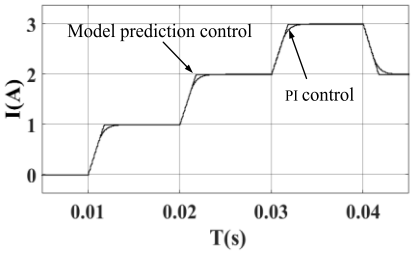

FIGURE 14. Five-axis system current response speeds with different control strategies.

different system stiffness were simulated and analyzed, as shown in Fig. 15 and Fig. 16, respectively. Fig. 12 shows the displacement response waveform in the case of $k = k_s$, and Fig. 13 shows the displacement response waveform in the case of $k = 1.2\ k_s$. A comparison between Fig. 12 and Fig. 13 shows that the two current control methods can achieve good results when the system stiffness is small. As the system stiffness was increased, the PI current control led to system instability, whereas the current control strategy based on the model prediction could maintain system stability.

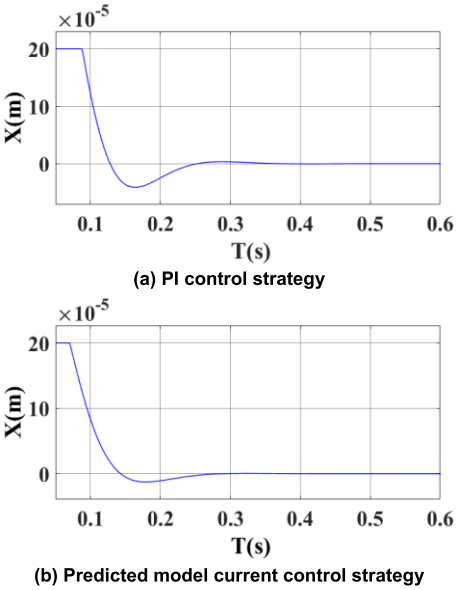

(a) PI control strategy

(b) Predicted model current control strategy

FIGURE 15. Response of displacement waveform when $k = k_s$.

B. TEST VERIFICATION

To verify the feasibility of the 5-axis system and its control strategy, a test platform was developed and set up. The system composition and equipment are shown in Fig. 17. The test platform was composed of a power amplifier, a controller, a position sensor, and a magnetic suspension motor; the test device parameters are shown in Tables 1 and 2.

The test results of the current response characteristics of the two control strategies are shown in Fig. 18. When the current reference value changed from 0 A to 4 A, both the PI control strategy and the predicted model current control

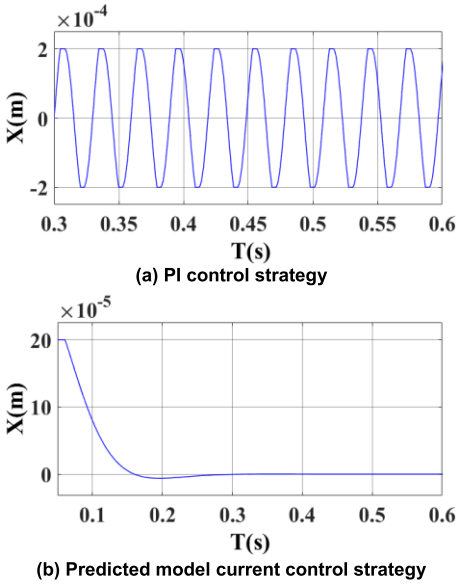

FIGURE 16. Response of displacement waveform when $k = 1.2k_s$.

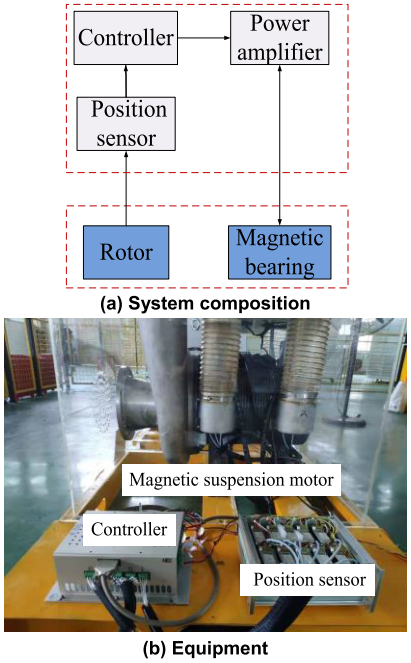

FIGURE 17. Active magnetic bearing test platform.

strategy could maintain the current reference value. However, the predicted model current control strategy had a better current response rate. In addition, the response time was reduced from 0.05 s to 0.01 s, which greatly increased the system response bandwidth.

The test results of the suspension position response characteristics with two different control modes and different system stiffnesses are shown in Fig. 19 and Fig. 20. In addition, the y-coordinate was 1 V at 100 u. It can be seen from the response waveform of the position that the predictive model

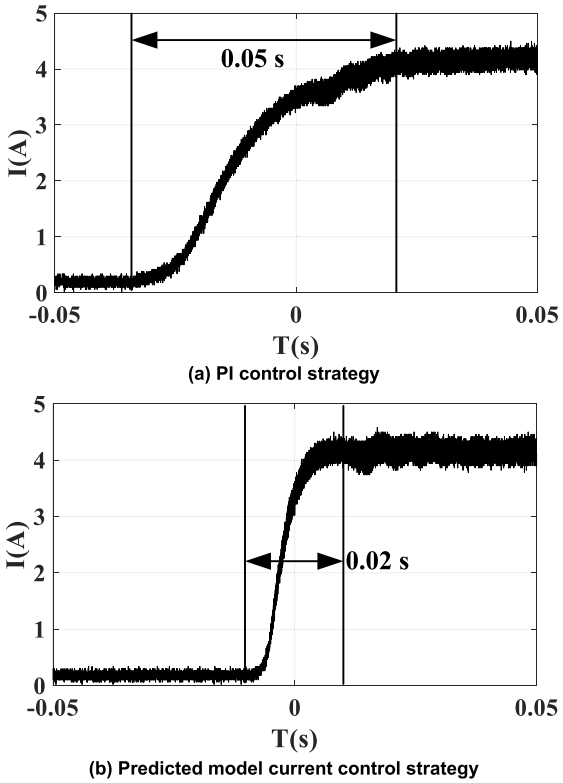

FIGURE 18. Current response speeds with different control strategies.

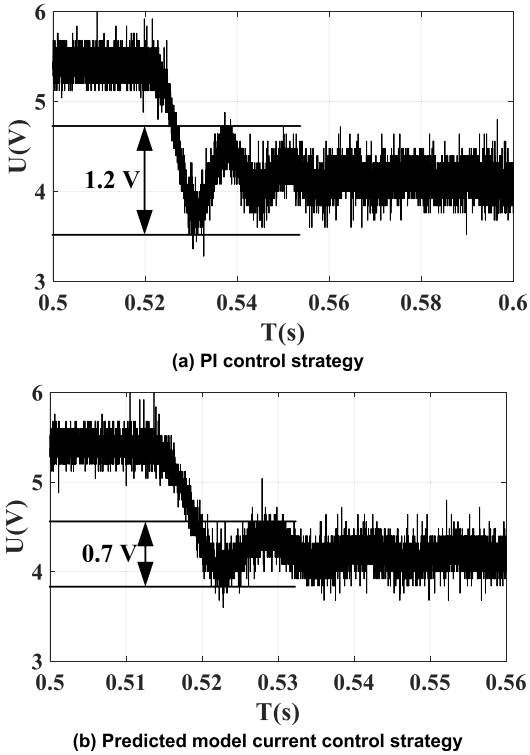

FIGURE 19. Response of displacement waveform when $k = k_s$.

current control strategy had better dynamic performance and better stability. Fig. 19 shows that the position overshoot of the model-based control strategy is slightly reduced in the

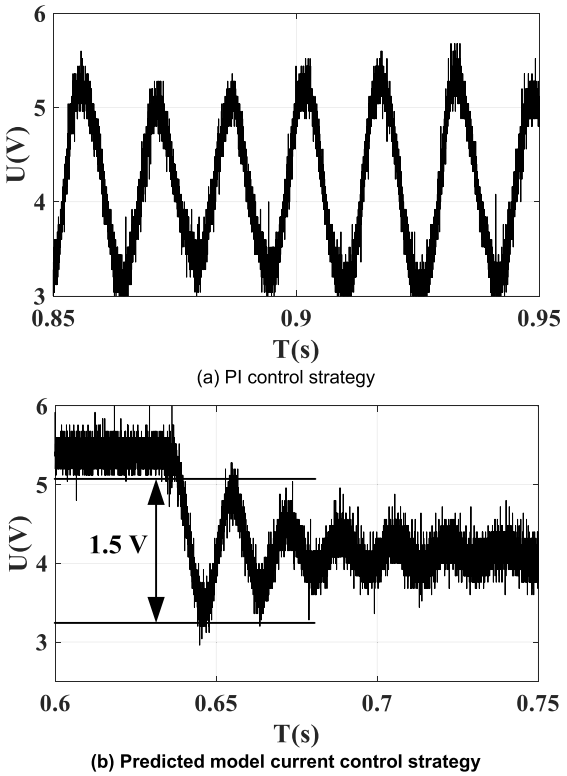

FIGURE 20. Response of displacement waveform when k=1.2k_s.

case of $k = k_s$. Fig. 20 shows the response waveform in the case of $k = 1.2\ k_s$, where the PI control is unstable, but the predictive model current control is still stable.

V. CONCLUSION

To optimize the performance of an active magnetic bearing system, this paper studied the topology of a switching power amplifier of an active magnetic bearing and the effect of switching power amplifier bandwidth on the system performance. Then, a new five-axis common bridge switching power amplifier topology and its corresponding optimal control strategy were proposed. Through simulations and experiments, relevant conclusions were drawn as follows:

1) A 5-axis common bridge switching power amplifier topology was proposed, in which the number of switching devices was reduced, and the power consumption of the switching power amplifier was decreased by 50% compared with the conventional topology.

2) Based on research on the topology and control stability, the maximum response speed of the current was $\max(di_L/dt) = aV_{dc}/L$, and the formula of the system stability was $k + k_s/D\omega_c < 1$. The above formulas could provide technical guidance for control parameter matching and system design.

3) The model-based current control method could improve system response speed compared to a PI control; i.e., the control strategy could increase the system bandwidth and stiffness under the same conditions, to ensure system stability.

REFERENCES

[1] G. Schweitzer, E. H. Maslen, H. Bleuler, and M. Cole, *Magnetic Bearings: Theory, Design, and Application to Rotating Machinery*. New York, NY, USA: Springer, 2010, pp. 21–78.
[2] A. Chiba, T. Fukao, O. Ichikawa, and M. Oshim, *Magnetic Bearings and Bearingless Drives*. Amsterdam, The Netherlands: Elsevier, 2005, pp. 38–64.
[3] T. Nussbaumer, P. Karutz, F. Zurcher, and J. W. Kolar, "Magnetically levitated slice motors-an overview," *IEEE Trans. Ind. Appl.*, vol. 47, no. 2, pp. 754–766, Mar./Apr. 2011.
[4] S. Carabelli, F. Maddaleno, and M. Muzzarelli, "High-efficiency linear power amplifier for active magnetic bearings," *IEEE Trans. Ind. Electron.*, vol. 47, no. 1, pp. 17–24, Feb. 2000.
[5] C. Liu, Z. Deng, C. Hua, and K. Li, "Design and implementation of a five-phase six-leg switching power amplifier for five degrees of freedom magnetic levitation bearing system," in *Proc. IEEE 8th Conf. Ind. Electron. Appl. (ICIEA)*, Melbourne, VIC, Australia, Jun. 2013, pp. 1254–1258.
[6] D. Jiang and P. Kshirsagar, "Analysis and control of a novel power electronics converter for active magnetic bearing drive," *IEEE Trans. Ind. Appl.*, vol. 53, no. 3, pp. 2222–2232, May 2017.
[7] H.-C. Hsieh, C.-W. Chen, M.-C. Chen, J.-S.-J. Lai, and J.-M. Lin, "Current spike suppression techniques for magnetic bearing amplifier," in *Proc. IEEE Appl. Power Electron. Conf. Expo. (APEC)*, Anaheim, CA, USA, Mar. 2019, pp. 17–21.
[8] D. Jiang, T. Li, Z. Hu, and H. Sun, "Novel topologies of power electronics converter as active magnetic bearing drive," *IEEE Trans. Ind. Electron.*, vol. 67, no. 2, pp. 950–959, Feb. 2020.
[9] C. Wei and D. Soffker, "Optimization strategy for PID-controller design of AMB rotor systems," *IEEE Trans. Control Syst. Technol.*, vol. 24, no. 3, pp. 788–803, May 2016.
[10] Z. Chen, Z. Lin, and Y. Li, "Output feedback control of an active magnetic bearing system based on adaptive command filtered backstepping," in *Proc. Chin. Control Conf. (CCC)*, Guangzhou, China, Jul. 2019, pp. 27–30.
[11] Y. Pinzhou, L. Hongwei, T. Jing, and Y. Wentao, "Influence of rotor vibration on magnetic field distribution of radial active magnetic bearings," in *Proc. 14th IEEE Conf. Ind. Electron. Appl. (ICIEA)*, Xi'an, China, Jun. 2019, pp. 19–21.
[12] X. Zhou, J. Fang, and S. Xu, "Analysis and suppression of the suspended rotor displacement fluctuation influence for motor system," *IEEE Trans. Ind. Electron.*, vol. 61, no. 12, pp. 6966–6974, Dec. 2014.
[13] A. Noshadi, J. Shi, W. S. Lee, P. Shi, and A. Kalam, "System identification and robust control of multi-input multi-output active magnetic bearing systems," *IEEE Trans. Control Syst. Technol.*, vol. 24, no. 4, pp. 1227–1239, Jul. 2016.
[14] T. Schuhmann, W. Hofmann, and R. Werner, "Improving operational performance of active magnetic bearings using Kalman filter and state feedback control," *IEEE Trans. Ind. Electron.*, vol. 59, no. 2, pp. 821–829, Feb. 2012.
[15] H. Sheh Zad, T. I. Khan, and I. Lazoglu, "Design and adaptive sliding-mode control of hybrid magnetic bearings," *IEEE Trans. Ind. Electron.*, vol. 65, no. 3, pp. 2537–2547, Mar. 2018.
[16] M. S. Kandil, M. R. Dubois, L. S. Bakay, and J. P. F. Trovao, "Application of second-order sliding-mode concepts to active magnetic bearings," *IEEE Trans. Ind. Electron.*, vol. 65, no. 1, pp. 855–864, Jan. 2018.
[17] Z. Su, D. Wang, J. Chen, X. Zhang, and L. Wu, "Improving operational performance of magnetically suspended flywheel with PM-biased magnetic bearings using adaptive resonant controller and nonlinear compensation method," *IEEE Trans. Magn.*, vol. 52, no. 7, Jul. 2016, Art. no. 8300304.
[18] T.-J. Su, W.-P. Kuo, V.-N. Giap, H. Q. Vu, and Q.-D. Nguyen, "Active magnetic bearing system using PID-surface sliding mode control," in *Proc. 3rd Int. Conf. Comput. Meas. Control Sensor Netw. (CMCSN)*, Matsue, Japan, May 2016, pp. 5–8.
[19] M. Fekry, A. M. Mohamed, and M. Fanni, "An intelligent Q-parameterization control design that captures non-linearity and fuzziness of uncertain magnetic bearing system," in *Proc. IEEE Conf. Control Appl. (CCA)*, Sydney, NSW, Sep. 2015, pp. 1078–1083.
[20] Z. Z. Su, D. Wang, L. T. Wu, and K. Wang, "Identification and mixed-sensitivity H_∞ control of permanent magnet biased axial magnetic bearing with multiple air gaps," in *Proc. IEEE Int. Conf. Appl. Supercond. Electromagn. Devices (ASEMD)*, Shanghai, China, Nov. 2015, pp. 248–250.

YAPING HE is currently pursuing the Ph.D. degree with the College of Electrical Engineering, Zhejiang University, China.

His research interests include power electronics and motor drives. He currently focuses on the research of novel converter topology and drive for active magnetic bearing.

XI HE received the M.S. degree in electrical engineering from Hunan University, China, in 2018. He is currently working at Zhuzhou CRRC Times Electric Co., Ltd.

His research interests include power electronics and active magnetic bearing.

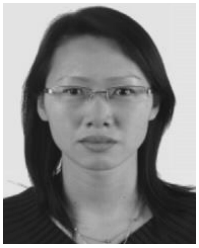

JIEN MA received the B.Eng. degree in mechatronics from Yanshan University, Qinhuangdao, China, in 2003, and the Ph.D. degree in electromechanics from Zhejiang University, Hangzhou, China, in 2009.

She is currently a Lecturer with the College of Electrical Engineering, Zhejiang University. Her research interests include electrical machines and drives, including permanent-magnet machines and cooling system design, mechatronics machines, and magneto fluid bearings.

YOUTONG FANG is currently a Professor with Zhejiang University, China, where he is working on electrical machines and drives. His research interests include PM machines and reliability analysis. He is a Fellow of IET.